A thermal theory for unifying and designing transparency, concentrating and cloaking

Ruizhe Wang, Liujun Xu, Qin Ji, and Jiping Huang

Citation: Journal of Applied Physics **123**, 115117 (2018); doi: 10.1063/1.5019306
View online: https://doi.org/10.1063/1.5019306
View Table of Contents: http://aip.scitation.org/toc/jap/123/11
Published by the American Institute of Physics

A thermal theory for unifying and designing transparency, concentrating and cloaking

Ruizhe Wang, Liujun Xu, Qin Ji, and Jiping Huang[a)]
Department of Physics, State Key Laboratory of Surface Physics, and Key Laboratory of Micro and Nano Photonic Structures (MOE), Fudan University, Shanghai 200433, China and Collaborative Innovation Center of Advanced Microstructures, Nanjing 210093, China

(Received 13 December 2017; accepted 7 March 2018; published online 20 March 2018)

In the existing literature of thermal metamaterials or metadevices, many properties or functions are designed via coordinate transformation theory (transformation thermotics), including thermal concentrating and cloaking. But other properties or functions, say, thermal transparency, are designed by using theories differing from the transformation thermotics. Here, we put forward an effective medium theory in thermotics by considering anisotropic layered/graded structures, and we reveal that the theory can unify transparency, concentrating, and cloaking into the same theoretical framework. Furthermore, the theory not only gives the criterion for transparency, concentrating, and cloaking, but also helps to predict a type of ellipses-embedded structures which can achieve transparency, concentrating, and cloaking, respectively. The prediction is confirmed by our finite-element simulations and/or experiments. This work provides a different theory to understand and design thermal metamaterials or metadevices, which might be extended to other disciplines, such as optics/electromagnetics and acoustics. *Published by AIP Publishing.*
https://doi.org/10.1063/1.5019306

I. INTRODUCTION

Since 2008, thermal metamaterials or metadevices[1–22] have been intensively studied, in order to achieve invisibility,[1–13] illusion[15–21] and other inconceivable thermal properties or functions, such as concentrators,[4,5,11,12] macroscopic diodes[10] and energy-free thermostats.[22]

On the one hand, most of the devices are designed based on the theory of coordinate transformation,[1–6,10–12,18–20] which originates from the pioneering work on electromagnetic waves in 2006.[23] For example, this theory helps to predict and realize the effect of thermal cloaking (which helps to let the heat flow around an object as if the object does not exist)[1–12] and concentrating (which corresponds to the concentration of heat in a specific region).[4,5,11,12]

On the other hand, some thermal metamaterials with other properties or functions are designed by using theories beyond transformation. Typically, thermal transparency (which means that heat flows across a region without disturbing the outside thermal signatures)[13,14] was proposed and designed by introducing the concept of neutral inclusion with computable effective thermal conductivities.

Here, we raise a question: does there exist a thermal theory which is capable of unifying thermal transparency, concentrating and cloaking into the same theoretical framework? If so, one would be able to design transparency, concentrating and cloaking from a different aspect, which may be convenient. Nevertheless, since thermal metamaterials with different properties or functions are composed of different structures and materials, it seems difficult to unify the theories. As an initial work, here, we attempt to overcome the difficulty through developing an effective medium theory in thermotics, which considers anisotropic layered/graded structures. Our simulations show that the theory can not only unify thermal transparency, concentrating and cloaking into the same theoretical framework, but also help to design practical devices on the basis of an ellipses-embedded structure according to the resulting theoretical criterion. The desired effects are confirmed by simulation and/or experiment.

II. THEORETICAL ANALYSIS OF TWO-DIMENSIONAL CIRCULAR STRUCTURES CONSTRUCTED BY ANISOTROPIC MATERIALS

A. Exact solution for a multi-layered structure

First of all, we consider a bilayer structure which is composed of two anisotropic materials [see Fig. 1(a)]. Their thermal conductivities are second-order diagonal tensors which have a radial element κ_{rr} (radial thermal conductivity) and a tangential element $\kappa_{\theta\theta}$ (tangential thermal conductivity). Considering the structure presented in a uniform thermal gradient field without heat sources, the conduction equation satisfies the Laplace equation

$$\nabla \cdot (-\boldsymbol{\kappa} \cdot \nabla T) = 0. \tag{1}$$

We conduct variable separation and derive the expression in polar coordinates since the thermal conductivity tensors have no items, $\kappa_{r\theta}$ and $\kappa_{\theta r}$. Then, we obtain

$$\frac{1}{r}\frac{\partial}{\partial r}\left(r\kappa_{rr}\frac{\partial T}{\partial r}\right) + \frac{1}{r}\frac{\partial}{\partial \theta}\left(\frac{\kappa_{\theta\theta}}{r}\frac{\partial T}{\partial \theta}\right) = 0. \tag{2}$$

The general solution of the above equation is

[a)]Electronic mail: jphuang@fudan.edu.cn

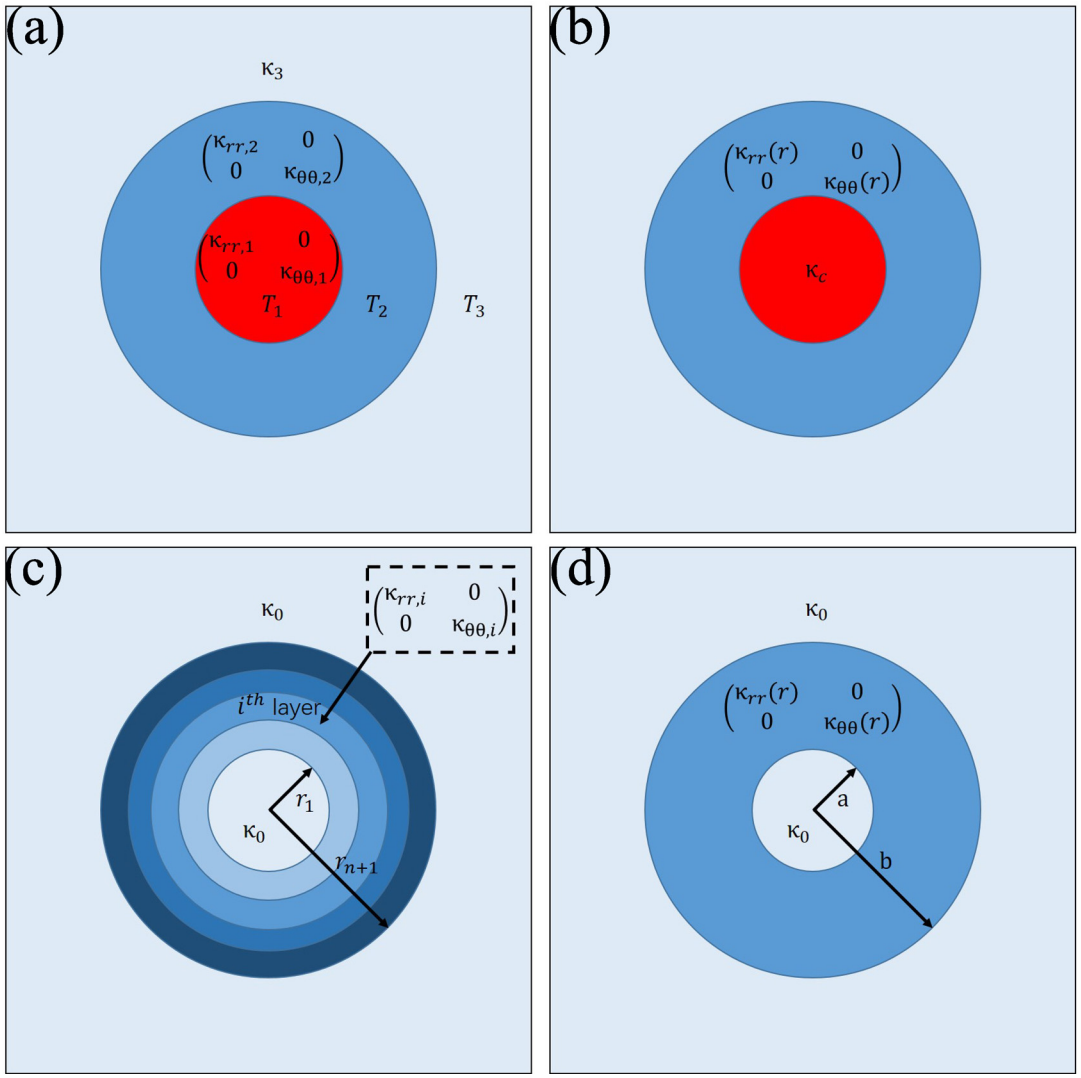

FIG. 1. Schematic diagram of (a) bilayer and (b) graded structures, (c) multi-layered and (d) graded rings. (a) For the bilayer structure, the circular core and the annular shell are composed of anisotropic materials, with radial ($\kappa_{rr,1}$ and $\kappa_{rr,2}$) and tangential ($\kappa_{\theta\theta,1}$ and $\kappa_{\theta\theta,2}$) thermal conductivities, respectively. (b) The graded structure is composed of a circular core with uniform thermal conductivity κ_c and an annular shell with radial ($\kappa_{rr}(r)$) and tangential ($\kappa_{\theta\theta}(r)$) thermal conductivities, respectively. The multi-layered ring in (c) is composed of n layers of concentric rings. The i-th ring with an inner radius r_i is composed of a material with radial ($\kappa_{rr,i}$) and tangential ($\kappa_{\theta\theta,i}$) thermal conductivities, respectively. The graded ring with an internal radius a and an external radius b is composed of a graded material with radial ($\kappa_{rr}(r)$) and tangential ($\kappa_{\theta\theta}(r)$) thermal conductivities, respectively.

$$T = A_0 + B_0 \ln r + \sum_{m=1}^{\infty} \left[A_m \cos(m\theta) + B_m \sin(m\theta)\right] r^m \sqrt{\frac{\kappa_{\theta\theta}}{\kappa_{rr}}} + \sum_{n=1}^{\infty} \left[C_n \cos(n\theta) + D_n \sin(n\theta)\right] r^{-n} \sqrt{\frac{\kappa_{\theta\theta}}{\kappa_{rr}}}. \quad (3)$$

When the structure shown in Fig. 1(a) is presented in a background with a thermal conductivity κ_3 and a uniform thermal gradient field ∇T (along the x direction), we can write the associated boundary conditions as

$$\begin{cases} T_1|_{r\to 0} \text{ is finite}, \\ T_1|_{r=r1} = T_2|_{r=r1}, \\ T_2|_{r=r2} = T_3|_{r=r2}, \\ -\kappa_{rr,1} \dfrac{\partial T_1}{\partial r}\Big|_{r=r1} = -\kappa_{rr,2} \dfrac{\partial T_2}{\partial r}\Big|_{r=r1}, \\ -\kappa_{rr,2} \dfrac{\partial T_2}{\partial r}\Big|_{r=r2} = -\kappa_3 \dfrac{\partial T_3}{\partial r}\Big|_{r=r2}, \\ T_3|_{r\to\infty} = -\nabla T r \cos\theta. \end{cases} \quad (4)$$

Here, T_1, T_2 and T_3 represent the temperature of the core, the shell and the background, respectively. Since the device is presented in an external temperature gradient along the x axis, the last boundary condition in Eq. (4) means that the thermal gradient field is uniform along the x axis ($r\cos\theta = x$) at infinity (the device cannot affect the temperature gradient at the infinity). Then, we can write down the solution of Eq. (2) by taking into account the boundary conditions

$$T_3 = \left(A_1 r + B_1 r^{-1}\right)\cos\theta. \quad (5)$$

Equation (5) partially keeps the first-order terms (m = 1 and n = 1) in Eq. (3) (general solution) to match the boundary conditions in Eq. (4). When the effective thermal conductivity of the structure (κ_e) is equal to that of the background (κ_3), there is no thermal contrast between the structure and the background. Hence, B_1 is expected to be zero. Thus, we obtain the effective thermal conductivity of the structure as

$$\kappa_e = c_2\kappa_{rr,2}\frac{(1+p^{c_2})c_1\kappa_{rr,1}+(1-p^{c_2})c_2\kappa_{rr,2}}{(1-p^{c_2})c_1\kappa_{rr,1}+(1+p^{c_2})c_2\kappa_{rr,2}}, \quad (6)$$

where $p = r_1^2/r_2^2$, $c_1 = \sqrt{\kappa_{\theta\theta,1}/\kappa_{rr,1}}$, and $c_2 = \sqrt{\kappa_{\theta\theta,2}/\kappa_{rr,2}}$. When $c_1 = c_2 = 1$ (isotropic material), Eq. (6) is reduced to the known Maxwell-Garnett theory.

So far, we have deduced the effective thermal conductivity of the bilayer circular structure which is composed of two anisotropic materials. For the multi-layered circular structure, we can firstly calculate the effective thermal conductivity (we define it as κ_{e1}) of the innermost two layers using the above conclusion. Then, by regarding the innermost two layers as one layer which possesses the uniform thermal conductivity of κ_{e1}, we can calculate the effective thermal conductivity of the innermost three layers. This procedure allows us to derive the effective thermal conductivity of the whole multi-layered structure by continuous iteration.

B. Exact solution for a graded structure

Based on the above deduction, our theory can also be extended into calculating the effective thermal conductivity of a graded structure. The graded structure is composed of a continuous medium whose anisotropic thermal conductivity varies along the radius. Consider a simple structure; see Fig. 1(b), which is composed of a homogeneous circular core (with a thermal conductivity of κ_c) and an anisotropic annular shell (with radial and tangential thermal conductivities of $\kappa_{rr}(r)$ and $\kappa_{\theta\theta}(r)$, respectively). By solving the Laplace equation, we obtain the effective thermal conductivity (κ_e) of the graded structure

$$\kappa_e = c\kappa_{rr}(r)\frac{(1+p^c)\kappa_c+(1-p^c)c\kappa_{rr}(r)}{(1-p^c)\kappa_c+(1+p^c)c\kappa_{rr}(r)}, \quad (7)$$

where p is the area fraction of the core and c is $\sqrt{\kappa_{\theta\theta}(r)/\kappa_{\pi}(r)}$. For convenience, we rewrite Eq. (7) as

$$\frac{\kappa_e-\kappa_{rr}(r)c}{\kappa_e+\kappa_{rr}(r)c} = p^c\frac{\kappa_c-\kappa_{rr}(r)c}{\kappa_c+\kappa_{rr}(r)c}. \quad (8)$$

For a shell with infinitesimal thickness of dr encircling the graded structure, the effective thermal conductivity changes from $\kappa_e(r)$ to $\kappa_e(r+\mathrm{d}r)$. In this case, Eq. (8) helps to obtain

$$\frac{\kappa_e(r+\mathrm{d}r)-\kappa_{rr}(r)c}{\kappa_e(r+\mathrm{d}r)+\kappa_{rr}(r)c} = \left[\frac{r^2}{(r+\mathrm{d}r)^2}\right]^c\frac{\kappa_e(r)-\kappa_{rr}(r)c}{\kappa_e(r)+\kappa_{rr}(r)c}. \quad (9)$$

As a result, we obtain a differential equation

$$\frac{\mathrm{d}\kappa_e(r)}{\mathrm{d}r} = \frac{[c\kappa_{rr}(r)]^2-\kappa_e(r)^2}{r\kappa_{rr}(r)}. \quad (10)$$

Given the gradation profiles [$\kappa_{rr}(r)$ and $\kappa_{\theta\theta}(r)$] and the boundary condition (when the radius is close to zero), the effective thermal conductivity of the whole graded structure, $\kappa_e(r)$, can be calculated according to Eq. (10).

C. Criterion for transparency, concentrating, and cloaking

So far, we have calculated the effective thermal conductivities of layered and graded structures which are composed of anisotropic materials. Based on these calculations, we are now in a position to provide the criterion for thermal transparency, concentrating and cloaking, and then these devices can be designed by using anisotropic materials accordingly. Let us consider two rings which are composed of multi-layered [Fig. 1(c)] and graded [Fig. 1(d)] anisotropic materials embedded in backgrounds with thermal conductivity κ_0. The following criteria hold true when $\kappa_{rr,i}\kappa_{\theta\theta,i} = \kappa_0^2$ (for multi-layered materials) and $\kappa_{rr}(r)\kappa_{\theta\theta}(r) = \kappa_0^2$ (for graded materials) are satisfied. Namely,

(1) When $\kappa_{rr}^{eff} = \kappa_{\theta\theta}^{eff}$, the structures shown in Figs. 1(c) and 1(d) are serving as thermal transparency devices.
(2) When $\kappa_{rr}^{eff} > \kappa_{\theta\theta}^{eff}$, the structures shown in Figs. 1(c) and 1(d) are serving as thermal concentrators.
(3) When $\kappa_{rr}^{eff} < \kappa_{\theta\theta}^{eff}$, the structures shown in Figs. 1(c) and 1(d) are serving as thermal cloaks. Especially, they tend to be perfect cloaks when $\kappa_{rr}^{eff} \to 0$.

Here, κ_{rr}^{eff} and $\kappa_{\theta\theta}^{eff}$ are the effective radial and tangential thermal conductivities, respectively. For the multi-layered structure described in Fig. 1(c), we have

$$\kappa_{rr}^{eff} = \ln\frac{r_{n+1}}{r_1}\left(\sum_{i=1}^{n}\frac{1}{\kappa_{rr,i}}\ln\frac{r_{i+1}}{r_i}\right)^{-1},$$
$$\kappa_{\theta\theta}^{eff} = \left(\ln\frac{r_{n+1}}{r_1}\right)^{-1}\sum_{i=1}^{n}\kappa_{\theta\theta,i}\ln\frac{r_{i+1}}{r_i}. \quad (11)$$

For the graded structure described in Fig. 1(d), we obtain

$$\kappa_{rr}^{eff} = \ln\frac{b}{a}\left(\int_a^b\frac{\mathrm{d}r}{\kappa_{rr}(r)r}\right)^{-1},$$
$$\kappa_{\theta\theta}^{eff} = \left(\ln\frac{b}{a}\right)^{-1}\int_a^b\frac{\kappa_{\theta\theta}(r)\mathrm{d}r}{r}. \quad (12)$$

III. THE DESIGN OF THERMAL TRANSPARENCY DEVICES, CONCENTRATORS AND CLOAKS VIA A FINITE-ELEMENT METHOD

According to the above theory, we firstly design two thermal transparency devices based on two-dimensional simulations by using the solid heat transfer module of commercial software COMSOL (https://www.comsol.com). The physics-controlled mesh is adjusted to be extremely fine in each simulation model. The left and right sides are fixed at constant temperatures playing the roles of heat and cold sources. The boundary conditions of the upper and bottom sides are heat insulated. Besides, in our simulations, the air convection is not considered. Figures 2(a) and 2(b) show the simulation results of an anisotropic [Fig. 2(a)] and a graded-anisotropic [Fig. 2(b)] annular device with an internal diameter of 2 cm and an external diameter of 4 cm embedded in square hosts with a side length of 9 cm. The basic parameters are described in the figure caption. To maintain uniform densities of the heat flux, the left sides of the hosts hold linear hot sources with a temperature of 323 K, and the right sides are linear cold sources with a temperature of 273 K. The color surfaces

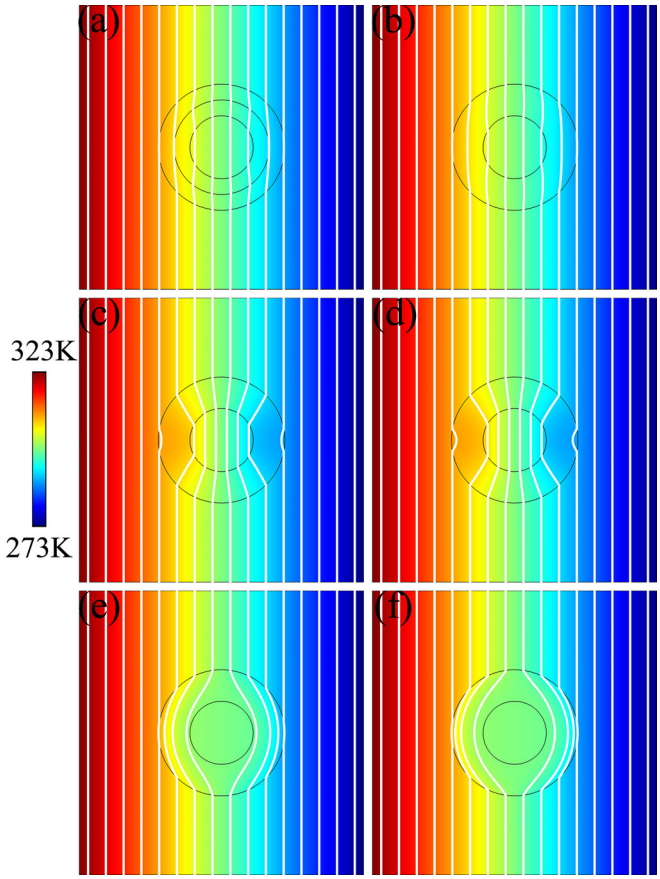

FIG. 2. Two-dimensional simulation results of [(a), (c), and (e)] anisotropic and [(b), (d), and (f)] graded-anisotropic thermal transparency devices, concentrators and cloaks presented in uniform backgrounds with a thermal conductivity of 30 W m^{-1}K^{-1}. (a) The anisotropic transparency device is composed of two layers of materials with the radial (36 W m^{-1}K^{-1} and 24.293 W m^{-1}K^{-1}) and tangential (25 W m^{-1}K^{-1} and 37.047 W m^{-1}K^{-1}) thermal conductivities, respectively. (b) The graded-anisotropic transparency device is composed of a graded material with the radial $\left(\frac{900}{(29ln2)r-1}\ \mathrm{W\,m^{-1}\,K^{-1}}\right)$ and tangential ($(29ln2)r - 1$ W m^{-1}K^{-1}) thermal conductivities, respectively. (c) The anisotropic concentrator is composed of a material with the radial (100 W m^{-1}K^{-1}) and tangential (9 W m^{-1}K^{-1}) thermal conductivities, respectively. (d) For the graded anisotropic concentrator, the ring is composed of a graded material with the radial ($100r - 30$ W m^{-1}K^{-1}) and tangential $\left(\frac{900}{100r-30}\ \mathrm{W\,m^{-1}\,K^{-1}}\right)$ thermal conductivities, respectively. The parameters of the two cloaks [(e) and (f)] are same as those used in the two concentrators [(c) and (d)], respectively, except for the interchanging parameters of tangential and radial thermal conductivities.

display the distribution of the temperature and white lines represent the isotherms. The isotherms inside and outside the devices are straight (which are not affected by the devices) as if there are no devices present in the backgrounds, demonstrating the behavior of thermal transparency.

Then, we further designed two thermal concentrators [Figs. 2(c) and 2(d)] and two thermal cloaks [Figs. 2(e) and 2(f)] which have the same geometrical parameters as those discussed in transparent devices. Figures 2(c) and 2(d) show the simulation results of an anisotropic [Fig. 2(c)] and a graded-anisotropic [Fig. 2(d)] thermal concentrator. The isotherms outside the devices are straight, reflecting the zero thermal contrast between the concentrators and the hosts. However, the isotherms inside the devices are bent and compressed to the center of the devices, exhibiting the phenomenon of thermal concentrating. Figures 2(e) and 2(f) show the simulation results of an anisotropic [Fig. 2(e)] and a graded-anisotropic [Fig. 2(f)] thermal cloak. In order to prevent the heat flux from entering the cloak regions, the tangential thermal conductivities are set to be much larger than the radial ones. The straight isotherms inside the devices reflect that the outer temperature gradients can hardly affect the cloak regions as the heat flows around the inner cloak regions through the anisotropic media.

IV. THE DESIGN OF THERMAL TRANSPARENCY DEVICES, CONCENTRATORS AND CLOAKS BASED ON ELLIPSES-EMBEDDED STRUCTURES

A. Thermal transparency device based on an ellipses-embedded structure

By taking advantage of the geometrical anisotropy of the air ellipses, we further design a thermal transparency device based on an ellipses-embedded structure; see Figs. 3(b)–3(d), verifying the above theory in both experiment and simulation. The thermal transparency device is composed of four concentric rings with multiple air ellipses embedded. The basic parameters of the structure are depicted in the figure caption. According to Ref. 21, we can achieve the effective thermal conductivity of a two-dimensional ellipse-embedded square host along the i-th axis of the ellipse

$$\kappa_i = \kappa_n \frac{[p + (1-p)L_i]\kappa_m + (1-p)(1-L_i)\kappa_n}{(1-p)L_i\kappa_m + [p + (1-p)(1-L_i)]\kappa_n}. \quad (13)$$

Here, we consider a binary composite where an air ellipse of thermal conductivity κ_m and area fraction p is embedded in a host medium of κ_n, in the presence of a uniform external thermal gradient field. To be mentioned, $L_i (i = a, b)$ is the shape factor of the two-dimensional ellipse, while a and b are the semi-axes of the air ellipses. We have

$$L_i = \frac{ab}{2}\int_0^\infty \frac{\mathrm{d}s}{(i^2+s)\sqrt{(a^2+s)(b^2+s)}}. \quad (14)$$

Then, we extend the above results into a two-dimensional ring which contains many air ellipses. It is easy to verify that as long as the distances between nearby ellipses are equal to the width of the ring and one of the axes of the air ellipses is set along the radius of the ring, the radial and tangential thermal conductivities of the ring can be approximately calculated by using Eq. (13). Thus, for the thermal transparency device depicted in Figs. 3(b)–3(d), the calculated results of the radial and tangential thermal conductivities of the four rings are 68 W m^{-1}K^{-1} and 101 W m^{-1}K^{-1}, respectively. Hence, the effective thermal conductivity of the whole device can be obtained by utilizing the above theory, which is equal to 84 W m^{-1}K^{-1}.

In addition, we also conduct an experiment to verify the above calculation. The sample [Fig. 3(b)] is fabricated by chemical etching of a 0.03 cm brass board with a thermal conductivity of 109 W m^{-1}K^{-1}, and a 0.1 mm-thick polydimethylsiloxane film is covered on the sample in order to eliminate the infrared reflection. A plastic foam board with

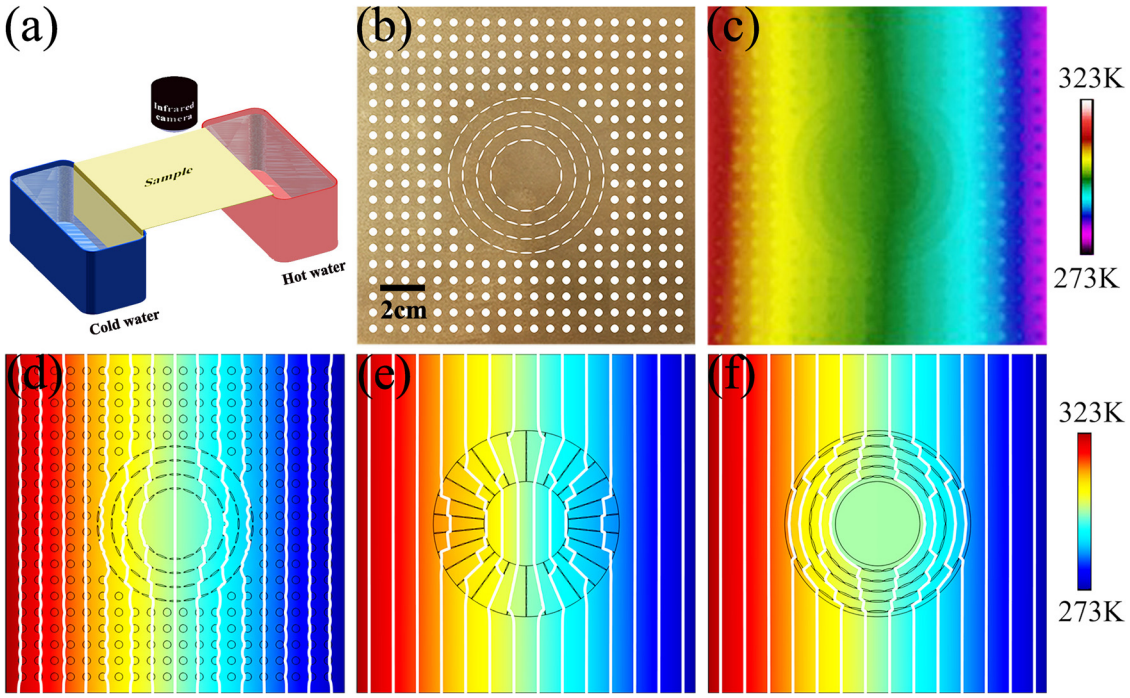

FIG. 3. Experimental (a) setup and (b) sample of the thermal transparency device. The transparency device is composed of 100 air ellipses, each with the major (minor) semi-axis of 0.33 cm (0.04 cm), which are drilled in the brass of 109 W $m^{-1}K^{-1}$. The distance between nearby ellipses equals 0.83 cm. The host background is occupied by a brass drilled with 312 air circles with a radius of 0.23 cm, providing a thermal conductivity of 80 W $m^{-1}K^{-1}$. Two-dimensional experimental and simulation results of ellipses-embedded structures: [(c) and (d)] thermal transparency device, (e) concentrator, and (f) cloak. (c) shows the experimental result of a transparency device and (d) is the simulation result corresponding to (c). (e) shows the simulation result of the concentrator in the presence of a uniform background with the thermal conductivity of 120 W $m^{-1}K^{-1}$. The concentrator is composed of five layers of air ellipses, each with the major (minor) semi-axis of 0.3 cm (0.03 cm), which are embedded in the background of 270 W $m^{-1}K^{-1}$. The width of the concentrator equals 3 cm. (f) shows the simulation result of the thermal cloak. The cloak is composed of five layers of air ellipses embedded in the background of 380 W $m^{-1}K^{-1}$; their major semi-axes are 0.3 cm, 0.355 cm, 0.415 cm, 0.48 cm and 0.54 cm, respectively, and their minor semi-axes are all 0.05 cm. Other parameters are the same as those used in (c).

the same size of sample is stuck on the back of the sample in order to weaken the air convection. Two water tanks, which are, respectively, filled with hot and ice water [shown in Fig. 3(a)], serve as heat and cold sources, respectively. The room temperature is tuned to be the middle temperature between the heat and cold sources, which can minimize the air convection. Then, we use an FLIR E60 infrared camera with a resolution of 240×240 pixels to detect the temperature profile. The experimental result is displayed in Fig. 3(c). The straight isotherms reflect that there is no thermal contrast between the device and the host background; that is to say, the effective thermal conductivity of the device is the same as that of the background. In the experiment, the thermal conductivity of the background is set to 80 W $m^{-1}K^{-1}$, which is nearly the same as the above calculated result. Figure 3(d) is the simulation result, which is consistent with the corresponding experimental result.

B. Thermal concentrator and cloak based on ellipses-embedded structures

By using the simulation method, we further design a thermal concentrator and a cloak with the radius of 5.5 cm based on the ellipses-embedded structures. To be different from the above equidistant distribution of the air ellipses, the air ellipses are equal-angle-distributed in the annular structures. The detailed parameters are described in the figure caption. Figures 3(e) and 3(f) show the two-dimensional simulation results of the thermal concentrator and the cloak. The white isotherms clearly show that the thermal concentrating [Fig. 3(e)] and cloaking effects [Fig. 3(f)] are achieved. In principle, the thermal concentrator and the cloak can be experimentally fabricated on the basis of the two designs. However, the thermal contact resistance of the welded junctions (which connect different materials) must be carefully eliminated, in order to keep the performance of the samples.

V. CONCLUSION

To sum up, we have proposed an effective medium theory in thermotics, which allows us to unify transparency, concentrating and cloaking into the same theoretical framework. The resulting theoretical criterion has helped us to design transparency, concentrating and cloaking, and we have confirmed the three functions via finite-element simulations. Furthermore, with the aid of the theory, we have introduced an ellipses-embedded structure for transparency, concentrating and cloaking; the desired effects have been verified in simulations and/or experiment. Our theory and the corresponding ellipses-embedded structure may be applied to achieve other thermal metamaterials like rotators, which are practically and commercially available for potential applications. In addition, our theory, together with the criterion, might be extended to other disciplines, such as optics/electromagnetics and acoustics.

ACKNOWLEDGMENTS

We appreciate the useful discussion with Mr. J. Shang. We acknowledge the financial support by the National Natural Science Foundation of China under Grant No. 11725521, and the Science and Technology Commission of Shanghai Municipality under Grant No. 16ZR1445100.

[1]C. Z. Fan, Y. Gao, and J. P. Huang, "Shaped graded materials with an apparent negative thermal conductivity," Appl. Phys. Lett. **92**, 251907 (2008).
[2]T. Chen, C.-N. Weng, and J.-S. Chen, "Cloak for curvilinearly anisotropic media in conduction," Appl. Phys. Lett. **93**, 114103 (2008).
[3]J. Y. Li, Y. Gao, and J. P. Huang, "A bifunctional cloak using transformation media," J. Appl. Phys. **108**, 074504 (2010).
[4]S. Guenneau, C. Amra, and D. Veynante, "Transformation thermodynamics: Cloaking and concentrating heat flux," Opt. Express **20**, 8207 (2012).
[5]S. Narayana and Y. Sato, "Heat flux manipulation with engineered thermal materials," Phys. Rev. Lett. **108**, 214303 (2012).
[6]R. Schittny, M. Kadic, S. Guenneau, and M. Wegener, "Experiments on transformation thermodynamics: Molding the flow of heat," Phys. Rev. Lett. **110**, 195901 (2013).
[7]H. Y. Xu, X. H. Shi, F. Gao, H. D. Sun, and B. L. Zhang, "Ultrathin three-dimensional thermal cloak," Phys. Rev. Lett. **112**, 054301 (2014).
[8]T. C. Han, X. Bai, D. L. Gao, T. L. Thong, B. W. Li, and C. W. Qiu, "Experimental demonstration of a bilayer thermal cloak," Phys. Rev. Lett. **112**, 054302 (2014).
[9]Y. G. Ma, Y. C. Liu, M. Raza, Y. D. Wang, and S. L. He, "Experimental demonstration of a multiphysics cloak: Manipulating heat flux and electric current simultaneously," Phys. Rev. Lett. **113**, 205501 (2014).
[10]Y. Li, X. Y. Shen, Z. H. Wu, J. Y. Huang, Y. X. Chen, Y. S. Ni, and J. P. Huang, "Temperature dependent transformation thermotics: From switchable thermal cloaks to macroscopic thermal diodes," Phys. Rev. Lett. **115**, 195503 (2015).
[11]T. Y. Chen, C. N. Weng, and Y. L. Tsai, "Materials with constant anisotropic conductivity as a thermal cloak or concentrator," J. Appl. Phys. **117**, 054904 (2015).
[12]X. Y. Shen, Y. Li, C. R. Jiang, Y. S. Ni, and J. P. Huang, "Thermal cloak-concentrator," Appl. Phys. Lett. **109**, 031907 (2016).
[13]X. He and L. Z. Wu, "Thermal transparency with the concept of neutral inclusion," Phys. Rev. E **88**, 033201 (2013).
[14]L. W. Zeng and R. X. Song, "Experimental observation of heat transparency," Appl. Phys. Lett. **104**, 201905 (2014).
[15]T. C. Han, X. Bai, T. L. Thong, B. W. Li, and C. W. Qiu, "Full control and manipulation of heat signatures: Cloaking, camouflage and thermal metamaterials," Adv. Mater. **26**, 1731 (2014).
[16]T. Z. Yang, Y. Su, W. Xu, and X. D. Yang, "Transient thermal camouflage and heat signature control," Appl. Phys. Lett. **109**, 121905 (2016).
[17]T. Z. Yang, X. Bai, D. L. Gao, L. Z. Wu, B. W. Li, T. L. Thong, and C. W. Qiu, "Invisible sensors: Simultaneous sensing and camouflaging in multiphysical fields," Adv. Mater. **27**, 7752 (2015).
[18]Y. X. Chen, X. Y. Shen, and J. P. Huang, "Engineering the accurate distortion of an object's temperature-distribution signature," Eur. Phys. J. Appl. Phys. **70**, 20901 (2015).
[19]N. Q. Zhu, X. Y. Shen, and J. P. Huang, "Converting the patterns of local heat flux via thermal illusion device," AIP Adv. **5**, 053401 (2015).
[20]Q. W. Hou, X. P. Zhao, T. Meng, and C. L. Liu, "Illusion thermal device based on material with constant anisotropic thermal conductivity for location camouflage," Appl. Phys. Lett. **109**, 103506 (2016).
[21]S. Yang, L. J. Xu, R. Z. Wang, and J. P. Huang, "Full control of heat transfer in single-particle structural materials," Appl. Phys. Lett. **111**, 121908 (2017).
[22]X. Y. Shen, Y. Li, C. R. Jiang, and J. P. Huang, "Temperature trapping: Energy-free maintenance of constant temperatures as ambient temperature gradients change," Phys. Rev. Lett. **117**, 055501 (2016).
[23]J. B. Pendry, D. Schurig, and D. R. Smith, "Controlling electromagnetic fields," Science **312**, 1780 (2006).